



# Synthesis and physical properties of tunable aryl alkyl ionic liquids based on 1-aryl-4,5-dimethylimidazolium cations

Stefan Fritsch and Thomas Strassner\*

## Full Research Paper

Open Access

Address:  
Physikalische Organische Chemie, Technische Universität Dresden,  
01062 Dresden, Germany

*Beilstein J. Org. Chem.* **2024**, *20*, 1278–1285.  
<https://doi.org/10.3762/bjoc.20.110>

Email:  
Thomas Strassner\* - [thomas.strassner@tu-dresden.de](mailto:thomas.strassner@tu-dresden.de)

Received: 04 March 2024  
Accepted: 16 May 2024  
Published: 31 May 2024

\* Corresponding author

Associate Editor: C. Stephenson

Keywords:  
conductivity; electrochemical window; ionic liquids; tunable aryl alkyl ionic liquid; viscosity

© 2024 Fritsch and Strassner; licensee  
Beilstein-Institut.  
License and terms: see end of document.

## Abstract

We present a new class of tunable aryl alkyl ionic liquids (TAAILs) based on 1-aryl-4,5-dimethylimidazolium cations with electron-withdrawing and -donating substituents in different positions of the phenyl ring and the bis(trifluoromethylsulfonyl)imide ( $\text{NTf}_2^-$ ) anion. We investigated the effect of additional methyl groups in the backbone of the imidazolium core on the physical properties regarding viscosity, conductivity and electrochemical window. With an electrochemical window of up to 6.3 V, which is unprecedented for TAAILs with an  $\text{NTf}_2^-$  anion, this new class of TAAILs demonstrates the opportunities that arise from modifications in the backbone of the imidazolium cation.

## Introduction

Ionic liquids (ILs) are a special class of solvents generally defined as salts with melting points below 100 °C [1]. Due to their unique properties, e.g., their high thermal stability and their negligible vapor pressure [2,3], ILs have found widespread use in different fields of chemistry like synthesis [4–9], catalysis [10–14] and materials science [15–23]. ILs generally consist of an organic cation [24], such as the imidazolium or ammonium ion and an inorganic anion like a halide anion or weakly coordinating anions like bis(trifluoromethylsulfonyl)imide  $[\text{NTf}_2^-]$  [25]. In addition, dicationic salts or anions containing metal complexes have been described [26,27]. Due to the numerous combinations of different anions and cations, ILs can also be described as designer solvents [28].

We introduced a new class of ionic liquids based on the 1-aryl-3-alkylimidazolium cation in 2009, the tunable aryl alkyl ionic liquids (TAAILs) [29]. This class of ionic liquids allows the modification of physical and chemical properties by variation of the functional groups present at the aryl ring of the ionic liquid in addition to the possibility to introduce alkyl chains with varying length [30]. TAAILs have already been successfully used for the synthesis of nanoparticles and as solvents in catalysis [31,32]. Recently we have described the synthesis and physical properties of TAAILs which have been blocked at the C2 position [33]. The use of a substituent at the C2 position was found to have a strong influence on the properties of these ionic liquids due to changes in the hydrogen-bonding network. Here,

we investigate the properties of TAAILs based on the 1-aryl-4,5-dimethylimidazolium cation. It is well known that the hydrogen atom at the C2 carbon atom of the imidazole core is more acidic than those in the C4/C5-position, where the methyl groups are expected to also have a significant effect on the molecular interactions. Platinum complexes using the 4,5-dimethylimidazole motif as a ligand were already reported by our group [34] and piqued our interest on the performance of TAAILs based on this motif. Since the introduction of methyl groups in the backbone of the imidazolium core increases the stability and basicity of the corresponding imidazolium derivatives [35–37], we wanted to investigate the impact on the properties of ILs. The negative impact on viscosity and conductivity due to the higher mass should be comparatively low. We investigated different substituents with electron-donating as well as electron-withdrawing properties at the aryl ring and the difference between the *ortho* and *para* position of the substituent on the properties of the IL. For the  $[NTf_2]^-$  salts of the TAAILs, the viscosity, conductivity and the electrochemical window were determined.

## Results and Discussion

In this work we focused on a synthetic strategy with cost efficient starting materials and a good scalability [38–42]. The substituted imidazoles **1–9** were synthesized using a

condensation reaction between the corresponding aniline and diacetyl monoxime (Scheme 1), since the condensation using diacetyl was not successful for electron-poor aniline derivatives.

This reaction leads to the formation of N-oxides, which were then reduced using iron powder. The imidazoles were synthesized in a one-pot procedure on a scale of up to 400 mmol. Quaternization of the imidazoles using bromoalkanes with different chain lengths provided the bromide salts **10–36**. Conversion to the  $NTf_2$  ionic liquids **37–63** was achieved via anion exchange using  $LiNTf_2$ .

The synthesized TAAILs with the  $NTf_2$  anion are all ionic liquids with a melting point well below 100 °C and the majority of these ILs can also be described as room temperature ionic liquids (RTIL), with a melting point below room temperature. The short-term thermal stability was investigated using ramped temperature analysis. The thermal decomposition temperatures (Table 1) for the ILs with the  $NTf_2$  anion are in the range from 266 °C (IL **59**) to 409 °C (IL **37**). In general, most ionic liquids with a butyl chain show higher decomposition temperatures than their counterparts with octyl or dodecyl chain. An increase in alkyl chain length from octyl to dodecyl, however, does not necessarily lead to a lower thermal stability.

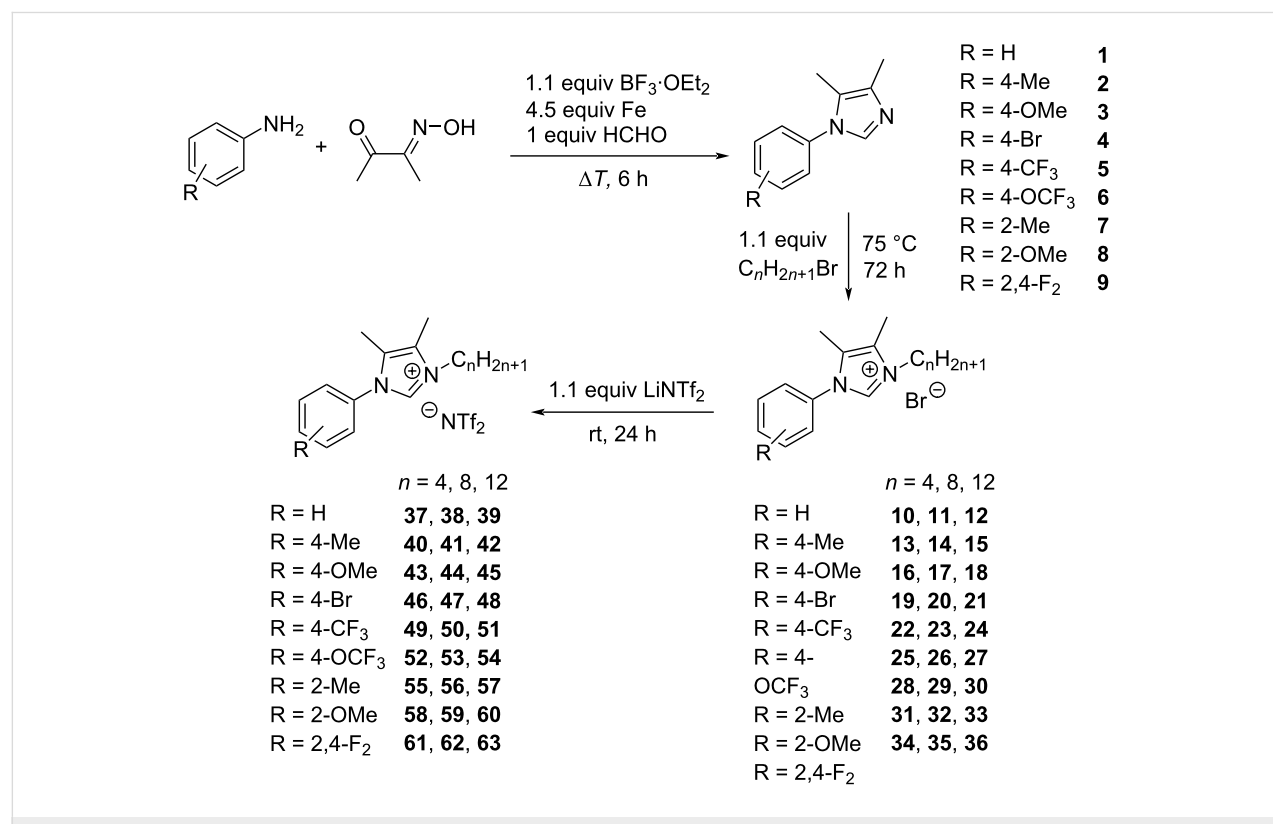


**Table 1:** Thermal decomposition point at 5% mass loss in °C for  $\text{NTf}_2^-$ -TAAILs **37–63** with different aryl substituents ( $R$ ) and alkyl chain lengths ( $n$ ).

$R$	$n = 4$	$n = 8$	$n = 12$
H	409	298	322
4-Me	396	349	316
4-OMe	300	306	363
4-Br	378	397	350
4-CF <sub>3</sub>	393	313	378
4-OCF <sub>3</sub>	383	370	307
2-Me	323	322	339
2-OMe	372	266	343
2,4-F <sub>2</sub>	398	364	291

With decomposition temperatures of up to 409 °C (IL **37**), the 1-aryl-4,5-dimethyl TAAILs can be described as ILs with a comparatively high thermal stability [43–45].

The viscosities of TAAILs with different aryl substitutions and a butyl chain are shown in Figure 1.

At 25 °C the highest measured viscosity was 1675 cP for the TAAIL with the 4-Br substitution and the lowest viscosity (521 cP) for the TAAIL with the unsubstituted aryl moiety. The

viscosities of the 4-CF<sub>3</sub> and 2,4-F<sub>2</sub> TAAILs with butyl chains are very similar, since the viscosity is influenced by  $\pi-\pi$  and dispersion effects facilitated by the electron-withdrawing effect of the fluorine atoms [46,47]. The 4-OCF<sub>3</sub> substituted TAAIL with a butyl chain, however, displayed a much lower viscosity, indicating that additional steric effects due to the 4-OCF<sub>3</sub> substituent play a role for the viscosity of the TAAIL [48,49]. The viscosities of the  $\text{NTf}_2$  ionic liquids **37–63** at 25 °C are given in Table 2. In general, with increasing alkyl chain lengths we observe an increasing viscosity of the TAAILs, which can be explained by the increase in molar mass and stronger van-der-Waals interactions. The only exceptions are the methoxy and 2,4-difluoro substituted TAAILs, demonstrating that the effects of the aryl substitution can have a stronger influence on the viscosity than the alkyl chain length.

The conductivity of the unsubstituted TAAIL **37** with 319  $\mu\text{S cm}^{-1}$  is the highest among the investigated 4,5-dimethylimidazolium based TAAILs (Figure 2, Table 3). This is supported by the corresponding observation that TAAIL **37** also shows the lowest viscosity. As a result of their high viscosity, the 4-Br substituted TAAILs **46** and **47** display the lowest conductivities (96 and 62  $\mu\text{S cm}^{-1}$ , respectively).

To visualize the correlation between conductivity and viscosity, the conductivity is plotted against the viscosity in Figure 3. The

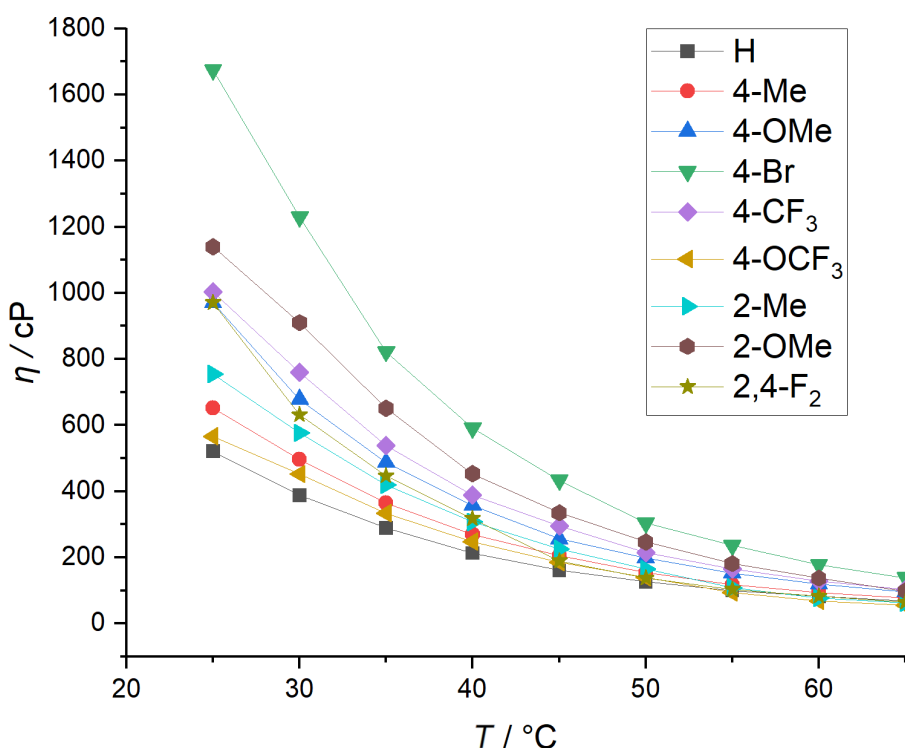


**Figure 1:** Temperature-dependent viscosity measurement of  $\text{NTf}_2^-$ -TAAILs **37–63** with a butyl chain and different aryl substitution  $R$ .

**Table 2:** Viscosity in centipoise (cP) of  $\text{NTf}_2^-$ -TAAILs 37–63 with different aryl substituents (R) and alkyl chain lengths (n), measured at 25 °C.

R	n = 4	n = 8	n = 12
H	521	570	683
4-Me	652	750	762
4-OMe	970	900	1020
4-Br	1675	1720	solid
4-CF <sub>3</sub>	1003	1092	solid
4-OCF <sub>3</sub>	566	638	solid
2-Me	755	835	919
2-OMe	1140	1134	1268
2,4-F <sub>2</sub>	971	891	1016

4-OCF<sub>3</sub> substituted TAAIL **52** shows a similar viscosity to TAAIL **37**, the conductivity, however, is much lower (198  $\mu\text{S cm}^{-1}$ ), demonstrating the influence of the perfluorinated 4-OCF<sub>3</sub> group on the conductivity.

Changing the position of the methyl and methoxy substituent from *ortho* to *para* leads to an increase in conductivity. Overall, longer alkyl chains lead to a decreasing conductivity, with the difference between butyl and octyl being more drastic than the difference between octyl and dodecyl.

To determine the electrochemical stability of the TAAILs, their electrochemical properties were investigated using linear sweep voltammetry (LSV, Figure 4). The setup consisted of a glassy carbon working electrode, a platinum wire counter electrode and a silver wire as reference electrode. The cutoff at which the cathodic limit  $E_{\text{red}}$  and the anodic limit  $E_{\text{ox}}$  were determined was  $-0.1$  and  $0.1 \text{ mA cm}^{-2}$ . The electrochemical window  $E_{\text{EW}}$  is determined from the difference between  $E_{\text{red}}$  and  $E_{\text{ox}}$ .

The anodic limit  $E_{\text{ox}}$  is mainly influenced by the anion of the ionic liquid, resulting in similar values for  $E_{\text{ox}}$  for the  $\text{NTf}_2^-$ -based TAAILs. The cathodic limit  $E_{\text{red}}$  depends on the cation and at what voltage the imidazolium cation is reduced. The substitution on the aryl ring has a strong influence on the reductive potential ( $E_{\text{red}}$ ), ranging from  $-0.7 \text{ V}$  for the 4-CF<sub>3</sub> substituted TAAIL **49** to  $-2.6 \text{ V}$  for the 2-Me substituted TAAIL **55** with a butyl chain. The change from *ortho* to *para* substitution led to a decrease of the cathodic limit in case of the methyl and methoxy-substituted TAAILs. The majority of TAAILs with a butyl chain have a cathodic limit between  $-1.0$  and  $-2.0 \text{ V}$ . The electrochemical window for the TAAILs with a butyl chain ranges from  $2.4 \text{ V}$  to  $4.4 \text{ V}$ . In general, an increase of the alkyl chain length leads to a wider electrochemical window. The results of the electrochemical measurements of all TAAILs can be found in Table 3, with the largest electrochemical window

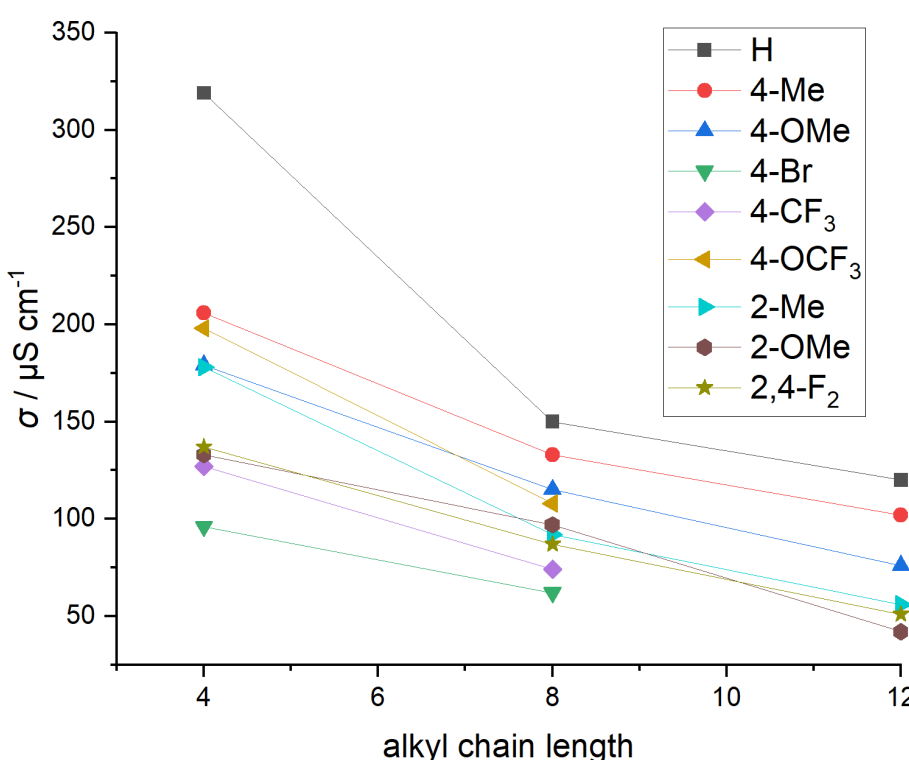


**Figure 2:** Conductivity of  $\text{NTf}_2^-$ -TAAILs 37–63 measured at 25 °C. Compounds **48**, **51**, and **54** are excluded because of their melting point.

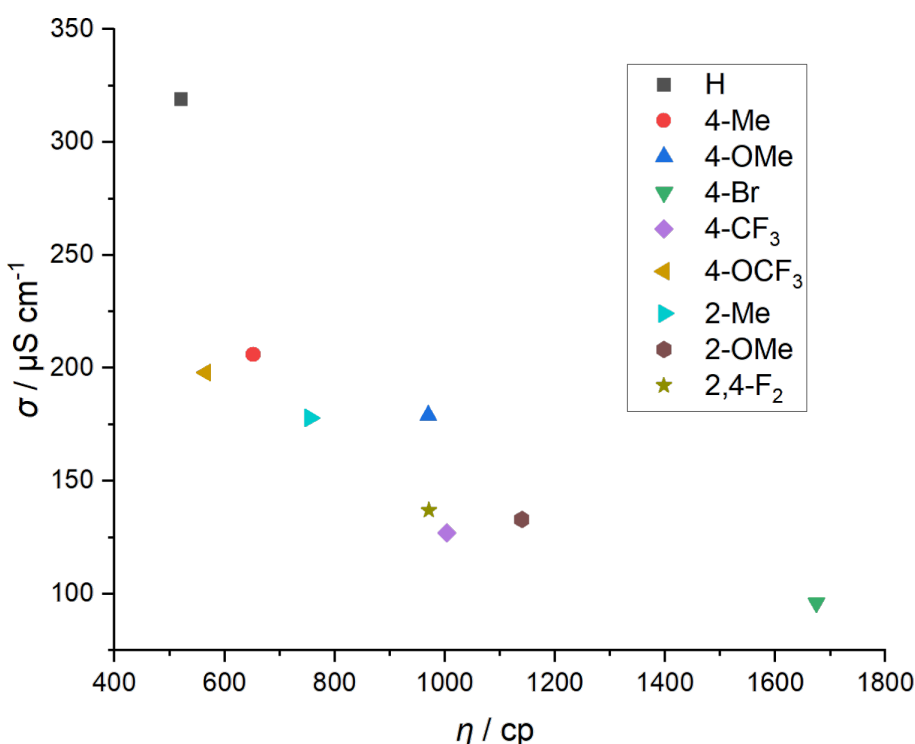


Figure 3: Conductivity of  $\text{NTf}_2^-$ -TAAILs with a butyl chain plotted against their viscosity at 25 °C.

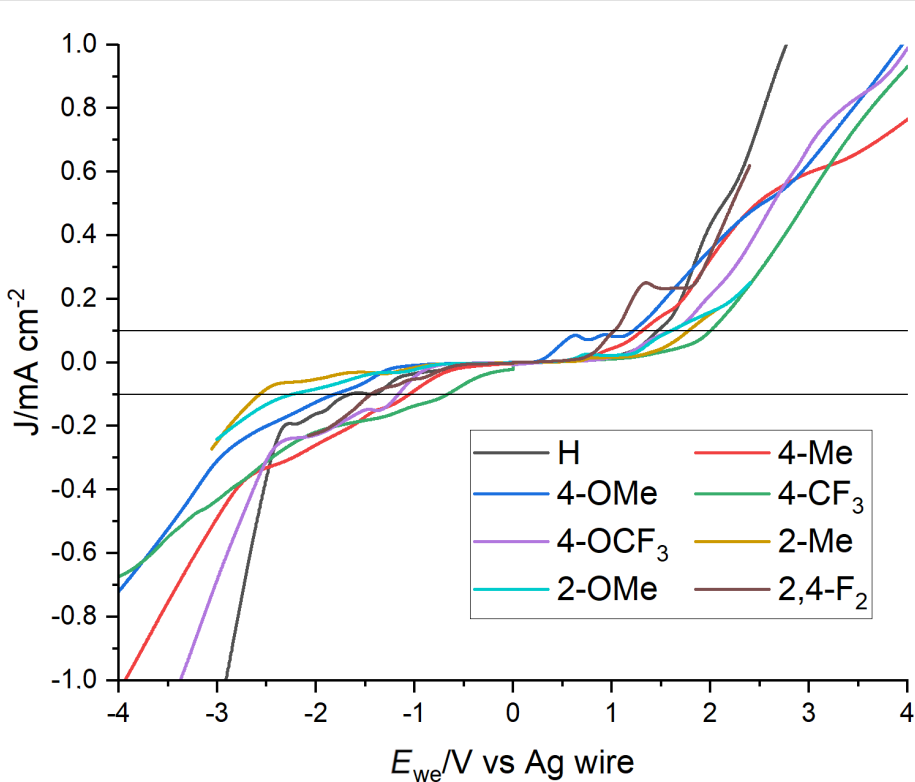


Figure 4: Linear sweep voltammetry of  $\text{NTf}_2^-$ -TAAILs with a butyl chain and different aryl substituents R. Black lines indicate cutoff. Scan rate: 50 mV s<sup>-1</sup>. Scan start at 0 V.

**Table 3:** Physicochemical data of  $\text{NTf}_2^-$ -TAAILs 37–63. R: aryl substituent, n: alkyl chain length. Specific conductivity  $\sigma$  was measured at 25 °C. Anodic and cathodic cut-off limit: 0.1 mA cm<sup>-2</sup>. 48, 51 and 54 are excluded due to their melting point.

Nr	R	n	$\sigma$ [ $\mu\text{S cm}^{-1}$ ]	$E_{\text{red}}$ [V]	$E_{\text{ox}}$ [V]	$E_{\text{EW}}$ [V]
37	H	4	319	-1.7	1.5	3.2
38	H	8	150	-2.0	1.6	3.6
39	H	12	120	-2.6	2.2	4.8
40	4-Me	4	206	-1.1	1.3	2.4
41	4-Me	8	133	-2.0	1.5	3.5
42	4-Me	12	102	-2.5	2.0	4.5
43	4-OMe	4	179	-1.8	1.2	3.0
44	4-OMe	8	115	-2.2	1.5	3.7
45	4-OMe	12	76	-3.0	1.7	4.7
46	4-Br	4	96	_a	_a	_a
47	4-Br	8	62	_a	_a	_a
49	4-CF <sub>3</sub>	4	127	-0.7	2.0	2.7
50	4-CF <sub>3</sub>	8	74	-2.9	2.3	5.2
52	4-OCF <sub>3</sub>	4	198	-1.2	1.6	2.8
53	4-OCF <sub>3</sub>	8	108	-2.9	2.6	5.5
55	2-Me	4	178	-2.6	1.8	4.4
56	2-Me	8	92	-2.7	2.2	4.9
57	2-Me	12	56	-3.4	2.9	6.3
58	2-OMe	4	133	-2.2	1.6	3.8
59	2-OMe	8	97	-2.7	1.9	4.6
60	2-OMe	12	42	-2.8	2.2	5.0
61	2,4-F <sub>2</sub>	4	137	-1.4	1.0	2.4
62	2,4-F <sub>2</sub>	8	87	-1.9	1.9	3.8
63	2,4-F <sub>2</sub>	12	51	-2.4	2.1	4.5

<sup>a</sup>No results due to decomposition.

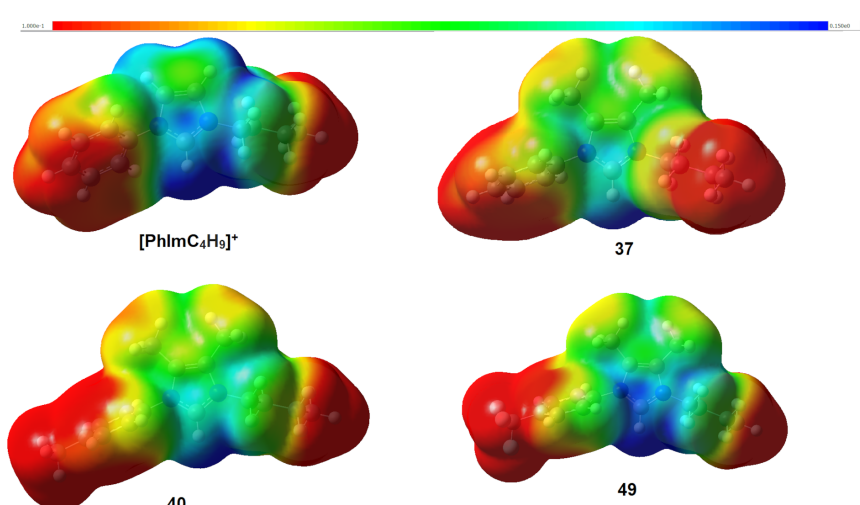
being 6.3 V for TAAIL **57**. This is the largest electrochemical window reported for TAAILs with  $\text{NTf}_2^-$  anion so far [50–53]. The size of the electrochemical window, however, depends heavily on the measurement conditions, preventing a general comparison with previously reported electrochemical windows [54,55]. The plots of all LSV measurements can be found in Supporting Information File 1 (Figures S1–S8).

Figure 5 shows the molecular electrostatic potential (MEP) of the unsubstituted TAAIL cation  $[\text{PhImC}_4\text{H}_9]^+$ , the unsubstituted 4,5-dimethyl-1-phenyl cation of TAAIL **37** and the cations of TAAILs **40** (4-CH<sub>3</sub>) and **49** (4-CF<sub>3</sub>).

The structures of the cations were optimized with Gaussian 16 [56], using the hybrid functional Becke3LYP [57–60] with the split valence triple- $\zeta$  basis set 6-311++G(d,p) [61–63] and D3 dispersion correction with the Becke–Johnson damping scheme [64,65]. All optimized structures were confirmed to be true minima by the absence of negative frequencies after harmonic vibrational modes calculation. The MEP was visualized with GaussView6. Comparing the 4,5-dimethylimidazolium cations **37**, **40** and **49** with the previously reported TAAIL cation  $[\text{PhImC}_4\text{H}_9]^+$  shows that the methyl groups in the backbone of the imidazolium cation lead to a different electrostatic potential (Figure 4). Comparison of the 4-Me substituted imidazolium cation **40** with the 4-CF<sub>3</sub> substituted cation **49** shows the influence of the electronegative fluorine atoms on the electrostatic potential of the cation.

## Conclusion

Based on the synthesis of nine different 1-aryl-4,5-dimethyl substituted imidazoles we report a new class of ionic liquids



**Figure 5:** Structures of the imidazolium cations obtained by DFT calculations (B3LYP/6-311++G (d,p)). The electrostatic potentials are indicated by color (blue: positive; red: negative).

with electron-donating and -withdrawing substituents, three different alkyl chain lengths and bromide as well as  $\text{NTf}_2$  anions. The physicochemical properties (thermal properties, viscosity, conductivity and electrochemical window) of the RTILs were investigated. The two methyl groups in the backbone of the imidazolium core lead to a slightly higher viscosity compared to the unsubstituted congeners. It is also influenced by the type of substitution (electron-withdrawing or -donating) at the aryl ring as well as the alkyl chain length. By introducing the methyl groups in the backbone of the imidazolium cation we were able to enlarge the electrochemical window up to 6.3 V, which is currently the largest window for a bis(trifluoromethylsulfonyl)imide tunable aryl alkyl ionic liquid.

## Supporting Information

### Supporting Information File 1

Experimental procedures and characterization data.  
[<https://www.beilstein-journals.org/bjoc/content/supplementary/1860-5397-20-110-S1.pdf>]

## Acknowledgements

The authors thank the ZIH Dresden for the generous allocation of compute time at their high-performance computing facility.

## ORCID® iDs

Thomas Strassner - <https://orcid.org/0000-0002-7648-457X>

## Data Availability Statement

All data that supports the findings of this study is available in the published article and/or the supporting information to this article.

## References

- Lei, Z.; Chen, B.; Koo, Y.-M.; MacFarlane, D. R. *Chem. Rev.* **2017**, *117*, 6633–6635. doi:10.1021/acs.chemrev.7b00246
- Brennecke, J. F.; Maginn, E. J. *AIChE J.* **2001**, *47*, 2384–2389. doi:10.1002/aic.690471102
- Wang, B.; Qin, L.; Mu, T.; Xue, Z.; Gao, G. *Chem. Rev.* **2017**, *117*, 7113–7131. doi:10.1021/acs.chemrev.6b00594
- Plechkova, N. V.; Seddon, K. R. *Chem. Soc. Rev.* **2008**, *37*, 123–150. doi:10.1039/b006677j
- Hallett, J. P.; Welton, T. *Chem. Rev.* **2011**, *111*, 3508–3576. doi:10.1021/cr1003248
- Ashraf, R.; Khalid, Z.; Sarfraz, A.; Bhatti, H. N.; Iqbal, M. A.; Nazari, V. *M. J. Mol. Struct.* **2021**, *1241*, 130701. doi:10.1016/j.molstruc.2021.130701
- Ghirardello, M.; Costantini, M.; Vecchi, A.; Pacifico, S.; Pazzi, D.; Castiglione, F.; Mele, A.; Marra, A. *Eur. J. Org. Chem.* **2022**, e202200100. doi:10.1002/ejoc.202200100
- Meeniga, I.; Gokanapalli, A.; Peddiahgari, V. G. R. *Sustainable Chem. Pharm.* **2022**, *30*, 100874. doi:10.1016/j.scp.2022.100874
- Zunita, M.; Wahyuningrum, D.; Buchari; Bundjali, B.; Gede Wenten, I.; Boopathy, R. *Bioresour. Technol.* **2020**, *315*, 123864. doi:10.1016/j.biortech.2020.123864
- Pârvulescu, V. I.; Hardacre, C. *Chem. Rev.* **2007**, *107*, 2615–2665. doi:10.1021/cr050948h
- Dupont, J.; Kollár, L., Eds. *Ionic Liquids (ILs) in Organometallic Catalysis; Topics in Organometallic Chemistry*; Springer Berlin: Berlin, Germany, 2015. doi:10.1007/978-3-662-47857-8
- Wasserscheid, P.; Keim, W. *Angew. Chem., Int. Ed.* **2000**, *39*, 3772–3789. doi:10.1002/1521-3773(20001103)39:21<3772::aid-anie3772>3.0.co;2-5
- Kumar, S.; Rastogi, S. K.; Singh, A.; Bharati Ahirwar, M.; Deshmukh, M. M.; Sinha, A. K.; Kumar, R. *Asian J. Org. Chem.* **2022**, *11*, e202100749. doi:10.1002/ajoc.202100749
- Tay, B.; van Meurs, M.; Tan, J.; Ye, S.; Borgna, A.; van Herk, A. M.; Selvaratnam, S.; Wang, C.; Taniguchi, S.; Suzuki, Y.; Utsunomiya, M.; Ito, M.; Monden, T.; Shibata, H.; Tomita, S. *Ind. Eng. Chem. Res.* **2021**, *60*, 17928–17941. doi:10.1021/acs.iecr.1c03822
- Galiński, M.; Lewandowski, A.; Stepiak, I. *Electrochim. Acta* **2006**, *51*, 5567–5580. doi:10.1016/j.electacta.2006.03.016
- Armand, M.; Endres, F.; MacFarlane, D. R.; Ohno, H.; Scrosati, B. *Nat. Mater.* **2009**, *8*, 621–629. doi:10.1038/nmat2448
- Drücker, P.; Rühling, A.; Grill, D.; Wang, D.; Draeger, A.; Gerke, V.; Glorius, F.; Galla, H.-J. *Langmuir* **2017**, *33*, 1333–1342. doi:10.1021/acs.langmuir.6b03182
- Ghaed-Sharaf, T.; Ghatee, M. H. *J. Mol. Liq.* **2021**, *332*, 115874. doi:10.1016/j.molliq.2021.115874
- Liwerska-Bizukojc, E.; Maton, C.; Stevens, C. V.; Gendaszewska, D. *J. Chem. Technol. Biotechnol.* **2014**, *89*, 763–768. doi:10.1002/jctb.4187
- Min, Z.; Chang, B.; Shao, C.; Su, X.; Wang, N.; Li, Z.; Wang, H.; Zhao, Y.; Fan, M.; Wang, J. *Appl. Catal., B* **2023**, *326*, 122185. doi:10.1016/j.apcatb.2022.122185
- Starling, P. D. J.; Metilda, P. J. *Mol. Struct.* **2022**, *1251*, 132062. doi:10.1016/j.molstruc.2021.132062
- Yang, Y.; Zhou, H.; Xiao, Y.; Feng, L.; Yang, L.; Mu, W.; Peng, X.; Bao, L.; Wang, J. *Carbohydr. Polym.* **2021**, *255*, 117363. doi:10.1016/j.carbpol.2020.117363
- Prete, D.; Dimaggio, E.; Demontis, V.; Zannier, V.; RodriguezDouton, M. J.; Guazzelli, L.; Beltram, F.; Sorba, L.; Pennelli, G.; Rossella, F. *Adv. Funct. Mater.* **2021**, *31*, 2104175. doi:10.1002/adfm.202104175
- Vekariya, R. L. *J. Mol. Liq.* **2017**, *227*, 44–60. doi:10.1016/j.molliq.2016.11.123
- Krossing, I.; Raabe, I. *Angew. Chem., Int. Ed.* **2004**, *43*, 2066–2090. doi:10.1002/anie.200300620
- Mezzetta, A.; Guglielmero, L.; Mero, A.; Tofani, G.; D'Andrea, F.; Pomelli, C. S.; Guazzelli, L. *Molecules* **2021**, *26*, 4211. doi:10.3390/molecules26144211
- Guglielmero, L.; Mero, A.; Mezzetta, A.; Tofani, G.; D'Andrea, F.; Pomelli, C. S.; Guazzelli, L. *J. Mol. Liq.* **2021**, *340*, 117210. doi:10.1016/j.molliq.2021.117210
- Earle, M. J.; Seddon, K. R. *Pure Appl. Chem.* **2000**, *72*, 1391–1398. doi:10.1351/pac2000072071391
- Ahrens, S.; Peritz, A.; Strassner, T. *Angew. Chem., Int. Ed.* **2009**, *48*, 7908–7910. doi:10.1002/anie.200903399

30. Lerch, S.; Strassner, T. *Chem. – Eur. J.* **2021**, *27*, 15554–15557. doi:10.1002/chem.202102545
31. Woitassek, D.; Strothmann, T.; Biller, H.; Lerch, S.; Schmitz, H.; Song, Y.; Roitsch, S.; Strassner, T.; Janiak, C. *Molecules* **2023**, *28*, 405. doi:10.3390/molecules28010405
32. Schroeter, F.; Lerch, S.; Kaliner, M.; Strassner, T. *Org. Lett.* **2018**, *20*, 6215–6219. doi:10.1021/acs.orglett.8b02688
33. Biller, H.; Strassner, T. *Chem. – Eur. J.* **2023**, *29*, e202202795. doi:10.1002/chem.202202795
34. Stipurin, S.; Strassner, T. *J. Organomet. Chem.* **2023**, *1000*, 122785. doi:10.1016/j.jorgancem.2023.122785
35. Alder, R. W.; Allen, P. R.; Williams, S. J. *J. Chem. Soc., Chem. Commun.* **1995**, 1267. doi:10.1039/c39950001267
36. Kuhn, N.; Steimann, M.; Weyers, G. Z. *Naturforsch., B: J. Chem. Sci.* **1999**, *54*, 427–433. doi:10.1515/znb-1999-0401
37. Kunetskiy, R. A.; Čísařová, I.; Šaman, D.; Lypakalo, I. M. *Chem. – Eur. J.* **2009**, *15*, 9477–9485. doi:10.1002/chem.200901203
38. Shabalin, D. A.; Camp, J. E. *Org. Biomol. Chem.* **2020**, *18*, 3950–3964. doi:10.1039/d0ob00350f
39. Patel, G.; Dewangan, D. K.; Bhakat, N.; Banerjee, S. *Curr. Res. Green Sustainable Chem.* **2021**, *4*, 100175. doi:10.1016/j.crgsc.2021.100175
40. Mityanov, V. S.; Perevalov, V. P.; Tkach, I. I. *Chem. Heterocycl. Compd.* **2013**, *48*, 1793–1800. doi:10.1007/s10593-013-1210-8
41. Koutsoukos, S.; Becker, J.; Dobre, A.; Fan, Z.; Othman, F.; Philippi, F.; Smith, G. J.; Welton, T. *Nat. Rev. Methods Primers* **2022**, *2*, 49. doi:10.1038/s43586-022-00129-3
42. Matthews, R. P.; Welton, T.; Hunt, P. A. *Phys. Chem. Chem. Phys.* **2014**, *16*, 3238–3253. doi:10.1039/c3cp54672a
43. Cao, Y.; Mu, T. *Ind. Eng. Chem. Res.* **2014**, *53*, 8651–8664. doi:10.1021/ie5009597
44. Maton, C.; De Vos, N.; Stevens, C. V. *Chem. Soc. Rev.* **2013**, *42*, 5963–5977. doi:10.1039/c3cs60071h
45. Yu, G.; Zhao, D.; Wen, L.; Yang, S.; Chen, X. *AIChE J.* **2012**, *58*, 2885–2899. doi:10.1002/aic.12786
46. Böhm, H.-J.; Banner, D.; Bendels, S.; Kansy, M.; Kuhn, B.; Müller, K.; Obst-Sander, U.; Stahl, M. *ChemBioChem* **2004**, *5*, 637–643. doi:10.1002/cbic.200301023
47. Leroux, F. R.; Manteau, B.; Vors, J.-P.; Pazenok, S. *Beilstein J. Org. Chem.* **2008**, *4*, 13. doi:10.3762/bjoc.4.13
48. Klocker, J.; Karpfen, A.; Wolschann, P. *Chem. Phys. Lett.* **2003**, *367*, 566–575. doi:10.1016/s0009-2614(02)01786-4
49. Barrosse-Antle, L. E.; Bond, A. M.; Compton, R. G.; O'Mahony, A. M.; Rogers, E. I.; Silvester, D. S. *Chem. – Asian J.* **2010**, *5*, 202–230. doi:10.1002/asia.200900191
50. Lane, G. H. *Electrochim. Acta* **2012**, *83*, 513–528. doi:10.1016/j.electacta.2012.08.046
51. De Vos, N.; Maton, C.; Stevens, C. V. *ChemElectroChem* **2014**, *1*, 1258–1270. doi:10.1002/celc.201402086
52. Doblinger, S.; Donati, T. J.; Silvester, D. S. *J. Phys. Chem. C* **2020**, *124*, 20309–20319. doi:10.1021/acs.jpcc.0c07012
53. Chen, Y.; Liu, S.; Bi, Z.; Li, Z.; Zhou, F.; Shi, R.; Mu, T. *Green Energy Environ.* **2024**, *9*, 966–991. doi:10.1016/j.gee.2023.05.002
54. Ganczar, P.; Zorebski, E.; Dzida, M. *Electrochim. Commun.* **2021**, *130*, 107107. doi:10.1016/j.elecom.2021.107107
55. Piatti, E.; Guglielmero, L.; Tofani, G.; Mezzetta, A.; Guazzelli, L.; D'Andrea, F.; Roddar, S.; Pomelli, C. S. *J. Mol. Liq.* **2022**, *364*, 120001. doi:10.1016/j.molliq.2022.120001
56. Gaussian 16, Revision A.03; Gaussian, Inc.: Wallingford, CT, 2016.
57. Becke, A. D. *J. Chem. Phys.* **1993**, *98*, 5648–5652. doi:10.1063/1.464913
58. Lee, C.; Yang, W.; Parr, R. G. *Phys. Rev. B* **1988**, *37*, 785–789. doi:10.1103/physrevb.37.785
59. Vosko, S. H.; Wilk, L.; Nusair, M. *Can. J. Phys.* **1980**, *58*, 1200–1211. doi:10.1139/p80-159
60. Stephens, P. J.; Devlin, F. J.; Chabalowski, C. F.; Frisch, M. J. *J. Phys. Chem.* **1994**, *98*, 11623–11627. doi:10.1021/j100096a001
61. Krishnan, R.; Binkley, J. S.; Seeger, R.; Pople, J. A. *J. Chem. Phys.* **1980**, *72*, 650–654. doi:10.1063/1.438955
62. Clark, T.; Chandrasekhar, J.; Spitznagel, G. W.; Schleyer, P. V. R. *J. Comput. Chem.* **1983**, *4*, 294–301. doi:10.1002/jcc.540040303
63. Frisch, M. J.; Pople, J. A.; Binkley, J. S. *J. Chem. Phys.* **1984**, *80*, 3265–3269. doi:10.1063/1.447079
64. Grimme, S.; Antony, J.; Ehrlich, S.; Krieg, H. *J. Chem. Phys.* **2010**, *132*, 154104. doi:10.1063/1.3382344
65. Grimme, S.; Ehrlich, S.; Goerigk, L. *J. Comput. Chem.* **2011**, *32*, 1456–1465. doi:10.1002/jcc.21759

## License and Terms

This is an open access article licensed under the terms of the Beilstein-Institut Open Access License Agreement (<https://www.beilstein-journals.org/bjoc/terms>), which is identical to the Creative Commons Attribution 4.0 International License

(<https://creativecommons.org/licenses/by/4.0/>). The reuse of material under this license requires that the author(s), source and license are credited. Third-party material in this article could be subject to other licenses (typically indicated in the credit line), and in this case, users are required to obtain permission from the license holder to reuse the material.

The definitive version of this article is the electronic one which can be found at:

<https://doi.org/10.3762/bjoc.20.110>